Selection Intensity in Cellular Evolutionary Algorithms for Regular Lattices

Mario Giacobini, *Student Member, IEEE*, Marco Tomassini, Andrea G. B. Tettamanzi, and Enrique Alba

***Abstract*—In this paper, we present quantitative models for the selection pressure of cellular evolutionary algorithms on regular one- and two-dimensional (2-D) lattices. We derive models based on probabilistic difference equations for synchronous and several asynchronous cell update policies. The models are validated using two customary selection methods: binary tournament and linear ranking. Theoretical results are in agreement with experimental values, showing that the selection intensity can be controlled by using different update methods. It is also seen that the usual logistic approximation breaks down for low-dimensional lattices and should be replaced by a polynomial approximation. The dependence of the models on the neighborhood radius is studied for both topologies. We also derive results for 2-D lattices with variable grid axes ratio.**

***Index Terms*—Asynchronous dynamics, cellular evolutionary algorithms (cEAs), regular lattices, selection intensity, synchronous dynamics.**

I. Introduction

CELLULAR evolutionary algorithms (cEAs) use populations that are structured according to a lattice topology. The structure may also be an arbitrary graph, but more commonly it is a one-dimensional (1-D) or two-dimensional (2-D) grid. This kind of spatially structured EA has been introduced in [1] and [2]. A distinctive feature of cEAs is slow diffusion of good individuals through the population and, thus, for a given selection method, they are more explorative than panmictic (i.e., standard mixing population) EAs. These aspects have been found useful for multimodal and other kinds of problems (see, for instance, [3]). Cellular evolutionary algorithms have become popular because they are easy to implement on parallel hardware [4], [5]. However, it is clear that the search is performed by the model, not by its implementation. Thus, in this paper, we will focus on cEA models and on their properties without worrying about implementation issues.

Several results have appeared on selection pressure and convergence speed in cEAs. Sarma and De Jong performed empirical analyses of the dynamical behavior of cellular genetic algorithms (cGAs) [6], [7], focusing on the effect that the local selection method, and the neighborhood size and shape have on the global induced selection pressure. Rudolph and Sprave [8] have shown how cGAs can be modeled by a probabilistic automata network and have provided proofs of complete convergence to a global optimum based on Markov chain analysis for a model including a fitness threshold. Recently, Giacobini *et al.* [9] have successfully modeled the selection pressure curves in cEAs on 1-D ring structures. Also, a preliminary study of 2-D, torus-shaped grids has appeared in [10] and [11].

Our purpose here is to investigate in detail, selection pressure in 1-D and 2-D population structures for two kinds of dynamical systems: synchronous and asynchronous. These two kinds of systems differ in the policies used to update the population at every step of the search. Our main contribution, thus, lies in providing mathematical models for the different update policies (and several selection strategies) that more accurately predict the experimentally observed takeover time curves with simple difference equations describing the propagation of the best individual under probabilistic conditions.

The paper proceeds as follows. In Section II, we summarize the main features relevant to our study. We discuss the takeover time concept in Section III, followed in Section IV by the introduction of the background ideas sustaining our mathematical models. Section V contains a discussion on the limitations of directly applying the logistic model to cEAs. This justifies the necessity of new mathematical models that are developed in the next two sections, for a ring (Section VI) and for a torus (Section VII). In Section VIII, we validate our models experimentally for two standard selection mechanisms: binary tournament and linear ranking. Also, because of the high interest of rectangular toroidal structures for the population in cEAs, we devote Section IX to such shape to enlarge the spectrum of interest of this paper. We conclude our analysis by exploring the theoretical implications of changing the radius of the neighborhood in the considered models (Section X). Section XI offers our concluding remarks and future research lines.

II. Synchronous and Asynchronous cEAs

Let us begin with a description of how a cEA works. A cEA maintains a population whose individuals are spatially distributed in cells. Each cell is occupied by one individual; therefore, the terms *cell* and *individual* may be used interchangeably without possibility of confusion.

A cEA starts with the cells in a random state and proceeds by successively updating them using evolutionary operators, until a termination condition is met. Updating a cell in a cEA means

Manuscript received October 8, 2004; revised January 17, 2005. The work of M. Giacobini and M. Tomassini was supported in part by the Fonds National Suisse pour la Recherche Scientifique under Contract 200021-103732/1. The work of E. Alba was supported in part by the Spanish Ministry of Education and European FEDER under Contract TIC2002-04498-C05-02 (the TRACER Project, http://tracer.lcc.uma.es).

M. Giacobini and M. Tomassini are with the Information Systems Department, University of Lausanne, CP1 1015 Dorigny-Lausanne, Switzerland (e-mail: mario.giacobini@unil.ch; marco.tomassini@unil.ch).

A. G. B. Tettamanzi is with the Information Technologies Department, University of Milano, IT-26013 Crema, Italy (e-mail: andrea.tettamanzi@unimi.it).

E. Alba is with the Department of Computer Science, University of Málaga, ES-29071 Málaga, Spain (e-mail: eat@lcc.uma.es).

Digital Object Identifier 10.1109/TEVC.2005.850298

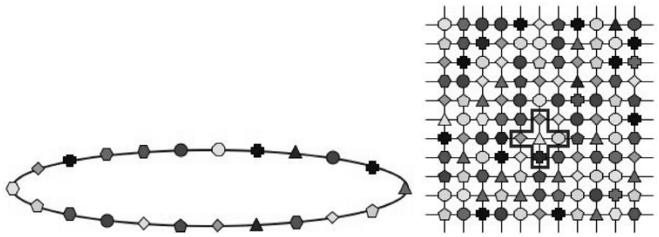

Fig. 1. (a) A ring cellular structure and (b) a grid cellular structure with a von Neumann neighborhood highlighted.

selecting two parents in the individual's neighborhood, applying genetic operators to them, and finally, replacing the individual if the obtained offspring has a better fitness (other replacement policies can also be used).

Before engaging in a description of the update policies, let us focus on the geographical distribution of the individuals themselves, a distinguishing feature of cEAs with respect to other population-based heuristics. Here, we consider cEAs defined on a 1-D lattice of size n or a square lattice of size $m \times m$, as depicted in Fig. 1. In this study, both the linear cEA, as well as the 2-D case have periodic boundary conditions, i.e., the structures are respectively a ring and a torus.

Let us call S the (finite) set of states that a cell can take up or, equivalently, the set of different individuals that can occupy a cell at any given time: this is the set of points in the (discrete) search space of the problem. Let K_i be the set of neighbors of a given cell i, and let $|K_i| = K$ be its size. Note that all the cells in the lattice have identical neighborhood geometry and size. The local transition function $\phi(\cdot)$ can then be defined as

$$\phi : S^K \rightarrow S$$

which maps the state $s_i \in S$ of a given cell i into another state from S, as a function of the states of the K cells in the neighborhood K_i. The main neighborhoods we consider in this paper are the *radius-one* neighborhood in the linear case, which comprises the cell itself and its first right and left neighbors and in the 2-D case, the von Neumann neighborhood, also called linear 5 ($|K_i| = 5$), which is constituted by the central cell and the four first neighbor cells in the directions north, east, south, and west (see Fig. 1). Thus, the implicit form of the stochastic transition function $\phi(\cdot)$ is

$$\phi(\cdot) = P\{x_i(t+1) \mid x_j(t) \in K_i\}$$

where P is the conditional probability that cell x_i will assume a certain value from the set S at the next time step $t+1$, given the current (time t) values of the states of all the cells in the neighborhood. We are, thus dealing with probabilistic automata [12], [13], and the set S should be seen as a set of values of a random variable. The probability P will be a function of the particular selection and variation methods.

With respect to time, cells can be updated either *synchronously* or *asynchronously*. In the synchronous case, all the cells change their states simultaneously, while in the asynchronous case cells are updated one at a time in some order.

The most mathematically satisfying asynchronous update method would be to use exponentially distributed waiting times, in which each cell has its own clock ticking according to an exponential distribution of mean λ [14]. This method is commonly used to simulate continuous time stochastic processes. Since we deal with finite-size populations evolving in discrete time steps here, we prefer to use step-based methods in which time is not explicitly defined.

There are many ways for sequentially updating the cells of a cEA. We consider four commonly used asynchronous update methods [15].

- In *fixed line sweep* (LS), the n cells are updated sequentially from left to right and line after line starting from the upper left corner cell.
- In *fixed random sweep* (FRS), the next cell to be updated is chosen with uniform probability without replacement; this will produce a certain update sequence $(c_1^j, c_2^k, \ldots, c_n^m)$, where c_q^p means that cell number p is updated at time q and $(j, k, \ldots, m)$ is a permutation of the n cells. The same permutation is then used for all update cycles.
- The *new random sweep* method (NRS) works like FRS, except that a new random cell permutation is used for each sweep through the array.[1]
- In *uniform choice* (UC), the next cell to be updated is chosen at random with uniform probability and with replacement. This corresponds to a binomial distribution for the updating probability.

A *time step* is defined as updating n times sequentially, which corresponds to updating *all* the n cells in the grid for LS, FRS, and NRS, and possibly less than n different cells in the uniform choice method, since some cells might be updated more than once.

III. Takeover Time

The *takeover time* is defined as being the time it takes for a single best individual to take over the entire population. It can be estimated experimentally by measuring the propagation of the proportion of the best individual under the effect of selection only, without any variation operator. Shorter takeover times indicate higher selection pressures and, thus, more exploitative algorithms. By lowering the selection intensity, the algorithm becomes more explorative. Theoretical takeover times have been derived by Deb and Goldberg [16] for panmictic populations and for the standard selection methods. These times turn out to be logarithmic in the population size, except in the case of proportional selection, which is a factor of n slower, where n is the population size.

It has been empirically shown in [6] that the selection pressure induced on the entire population becomes weaker as we move from a panmictic to a square grid population (both of the same size, with synchronous updating of the cells).

A study on the selection pressure in the case of ring and array topologies in 1-D cEAs has been done by Rudolph [17]. Abstracting from specific selection methods, he splits the selection procedure into two stages: in the first stage an individual is

[1]Note that over many sweeps the FRS method has a larger variance than the NRS since the FRS sequence could be an extremely favorable or defavorable one, while in NRS these effects would be smoothed out.

chosen in the neighborhood of each individual, and then, in the second stage, for each individual it is decided whether the previously chosen individual will replace it in the next time step. Using only replacement methods in which extinction of the best by chance cannot happen, i.e., nonextinctive selection, Rudolph derives the expected takeover times for the two topologies as a function of the population size and the probability that in the selection step the individual with the best fitness is selected in the neighborhood.

In this paper, we complete and extend the previous investigations to comprise synchronous and asynchronous cell update modes for 1-D and 2-D torii (i.e., rings and wrapped 2-D grids). In the next sections, we introduce quantitative models for the growth of the best individual in the form of difference stochastic equations.

IV. Mathematical Models

Let us consider the random variables $V_i(t) \in \{0,1\}$ indicating the presence in cell i ($1 \leq i \leq n$) of a copy of the best individual ($V_i(t)=1$) or of a worse one ($V_i(t)=0$) at time step t, where n is the the population size. The random variable

$$N(t) = \sum_{i=1}^{n} V_i(t)$$

denotes the number of copies of the best individual in the population at time step t. Initially, $V_i(1)=1$ for some individual i, and $V_j(1)=0$ for all $j \neq i$.

Following Rudolph's definition [17], if the selection mechanism is nonextinctive, the expectation $E[T]$ with

$$T = \min\{t \geq 1 : N(t) = n\}$$

is called the takeover time of the selection method. In the case of spatially structured populations, the quantity $E_i[T]$, denoting the takeover time if cell i contains the best individual at time step 1, is termed the takeover time with initial cell i. Assuming a uniformly distributed initial position of the best individual among all cells, the takeover time is, therefore, given by

$$E[T] = \frac{1}{n}\sum_{i=1}^{n} E_i[T].$$

In the following sections, we give the recurrences describing the growth of the random variable $N(t)$ in a cEA with different regular lattice topologies for the synchronous and the four asynchronous update policies described in Section II. We consider nonextinctive selection mechanisms that select the best individual in a given neighborhood with probabilities in the interval (0,1].

V. Limitations of the Logistic Modeling

It is well known since the work of Verhulst [18], that the assumption of logistic growth is a reasonable model for biological populations within bounded resources [19]. It is easy to see that this behavior also holds for the best individual growth in the artificial evolution of a finite-panmictic population [16]. In fact, if we consider a population of size n, the number $N(t)$ of copies of the best individual in the population at time step t is given by the following recurrence:

$$\begin{cases} N(0) = 1 \\ N(t) = N(t-1) + p_s N(t-1)(n - N(t-1)) \end{cases}$$

where p_s is the probability that the best individual is chosen. This recurrence can be easily transformed into one that describes a discrete logistic population growth in discrete time

$$\begin{cases} N(0) = 1 \\ N(t) = N(t-1) + (p_s n) N(t-1)\left(1 - \frac{1}{n} N(t-1)\right). \end{cases}$$

Such a recurrence can be approximated in analytical form by the standard continuous logistic equation[2]:

$$N(t) = \frac{n}{1 + \left(\frac{n}{N(0)} - 1\right) e^{-\alpha t}}$$

where the growth coefficient α depends on the probability p_s. This happens to be the approach taken in [7] for synchronous cEAs in order to fit the measured growth curves as a function of a single structural parameter.

This can be useful as a first approximation but, as suggested by Spiessens and Manderick [20], the growth of individuals propagation in a 2-D grid under local fitness-proportionate selection should follow a quadratic law. Gorges–Schleuter in [21], made similar remarks, noting that in the artificial evolution of locally interacting, spatially structured populations, the assumption of a logistic growth does not hold anymore.

Indeed, in these locally interacting structures, although the curves do have the familiar "S-shape" denoting growth followed by saturation, they are not exponential but rather polynomial with a time dependence $\propto t^d$, with d the lattice dimension.

In fact, in the case of a ring or a torus structure, we have, respectively, a linear and a quadratic growth. We complete here their analysis which holds for unrestricted growth, extending it to bounded synchronously updated spatial populations.

For a structured population, let us consider the limiting case, which represents an upper bound on growth rate, in which the selection mechanism is deterministic (i.e., where $p_s = 1$), and a cell always chooses its best neighbor for updating. If we consider a population of size n with a ring structure and a neighborhood radius of r (i.e., a neighborhood of a cell contains $2r+1$ cells), the following recurrence describes the growth of the number of copies of the best individual:

$$\begin{cases} N(0) = 1 \\ N(t) = N(t-1) + 2r \end{cases}.$$

This recurrence can be described by the closed equation $N(t) = N(0) + 2rt$, which clearly shows the linear character of the growth rate.

In the case of a population of size n disposed on a toroidal grid of size $\sqrt{n} \times \sqrt{n}$ (assuming $\sqrt{n}$ odd) and a von Neumann generalized neighborhood structure of radius r (see Section X),

[2]Note that this is not true in a rigorous sense. The discrete logistic map can give rise to chaotic behavior for a range of the parameters [19]. This is ignored in the previous qualitative discussion.

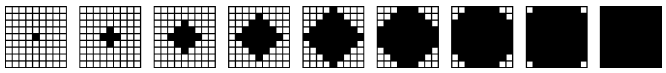

Fig. 2. Example of a deterministic growth of $N(t)$ for a population of 81 individuals on a 9×9 torus structure.

the growth of the number of copies of the best individual can be described by the following recurrence:

$$\begin{cases} N(0)=1 \\ N(t)=N(t-1)+4\sum_{i=0}^{r-1}(rt-i), & \text{for } 0\le t \le \frac{\sqrt{n}-1}{2} \\ N(t)=N(t-1)+4\sum_{i=0}^{r-1}(\sqrt{n}-rt-i), & \text{for } t> \frac{\sqrt{n}-1}{2} \end{cases}$$

which reduces to the first equation at the bottom of the page. This growth is described by a convex quadratic equation followed by a concave one, as the two closed forms of the recurrence clearly show in the second equation at the bottom of the page. Fig. 2 graphically depicts the growth described by the above equations for a population of 81 individuals disposed on a 9×9 torus structure using a radius 1 von Neumann neighborhood.

Thus, a more accurate fitting should take into account the nonexponential growth followed by saturation (crowding effect). We address such study in the following sections in the cases of 1-D and 2-D regular lattice topologies for synchronous and asynchronous evolution.

VI. Ring Structure

In a ring topology, each cell has the same number of neighbors on both sides, and this number depends on the *radius* r. We will first consider the simplest case $r = 1$, which means that there are three neighbors, including the central cell itself.

At each time step t, the expected number of copies $N(t)$ of the best individual is independent from its initial position. Therefore, the expected takeover time is $E[T] = E_i[T], \forall i$.

A. Synchronous Takeover Time

Since we consider neighborhoods of radius 1, the set of cells containing a copy of the best individual will always be a connected region of the ring. Therefore, at each time step, only two more cells (the two adjacent to the connected region of the ring) will contain a copy of the best individual with probability p. The growth of the quantity $N(t)$ can be described by the following recurrence:

$$\begin{cases} N(0) = 1 \\ E[N(t)] = \sum_{j=1}^{n} P[N(t-1) = j]\,(j+2p) \end{cases}$$

where $P[N(t-1) = j]$ is the probability that the random variable N has the value j at time step $t-1$. Since $\sum_{j=1}^{n} P[N(t-1) = j] = 1$, and the expected number $E[N(t-1)]$ of copies of the best individual at time step $t-1$ is by definition $\sum_{j=1}^{n} P[N(t-1) = j]\, j$, the previous recurrence is equivalent to

$$\begin{cases} N(0) = 1 \\ E[N(t)] = E[N(t-1)] + 2p. \end{cases}$$

The closed form of this recurrence is trivially

$$E[N(t)] = 2pt + 1$$

therefore, the expected takeover time $E[T]$ for a synchronous ring cEA with n cells is

$$E[T] = \frac{1}{2p}\,(n-1).$$

Rudolph [17] gave analytical results for the ring with synchronous update for a generic probability of selection p. Although obtained in a different way, the previous expression and his equation give nearly the same results for large population sizes n. In fact, his equation, for large n, reduces to $(n/2p) - (1/4)$, while our equation gives $(n/2p) - (1/2p)$. Given that the first term quickly dominates the second for large n, the two expressions are considered equivalent.

B. Asynchronous Fixed Line Sweep Takeover Time

Let us consider the general case of an asynchronous fixed line sweep cEA, in which the connected region containing the copies of the best individual at time step t is $B(t) = \{l, \ldots, k\}$, $1 < l \le k < n$. At each time step the cell $l-1$ will contain a copy of the best individual with probability p, while the cells $k+j$ (with $j = 1, \ldots, n-k$) will contain a copy of the best individual with probability p^j. The recurrence describing the growth of the random variable $N(t)$ is, therefore

$$\begin{cases} N(0) = 1 \\ E[N(t)] = \sum_{j=1}^{n} P[N(t-1) = j] \left(j + p + \sum_{i=1}^{n-j} p^i\right). \end{cases}$$

$$\begin{cases} N(0) = 1 \\ N(t) = N(t-1) + 4r^2t - 2r(r+1), & \text{for } 0 \le t \le \frac{\sqrt{n}-1}{2} \\ N(t) = N(t-1) - 4r^2t + 4r\sqrt{n} - 2r(r+1), & \text{for } t > \frac{\sqrt{n}-1}{2} \end{cases}$$

$$\begin{cases} N(t) = 2r^2t^2 + 2r(2r+1)t + 1, & \text{for } 0 \le t \le \frac{\sqrt{n}-1}{2} \\ N(t) = -2r^2t^2 + 2r(2\sqrt{n} - 3r - 1)t + 1, & \text{for } t > \frac{\sqrt{n}-1}{2} \end{cases}$$

Since $\sum_{i=1}^{n-j} p^i$ is a geometric progression, for large n we can approximate this quantity by the limit value $p/(1-p)$ of the summation. The recurrence is, therefore, equivalent to the following equation:

$$\begin{cases} N(0)=1 \\ E[N(t)]=E[N(t-1)]+p+\frac{p}{1-p} = E[N(t-1)] + \frac{2p-p^2}{1-p}. \end{cases}$$

The closed form of the previous recurrence being

$$E[N(t)] = \frac{2p-p^2}{1-p}\, t+1$$

we conclude that the takeover time for an asynchronous fixed line sweep cEA with a population of size n is

$$E[T] = \frac{1-p}{2p-p^2}(n-1).$$

C. Asynchronous Fixed and New Random Sweep Takeover Times

The mean behaviors of the two asynchronous fixed and new random sweep update policies among all the possible permutations for the sweeps are equivalent. We, therefore, give only one model describing the growth of the random variable $N(t)$ for both policies.

Let us again consider the general case in which the connected region containing the copies of the best individual at time step t is $B(t) = \{l,\ldots,k\}$ (with $1 < l \leq k < n$). The cells $l-1$ and $k+1$ have a probability p of containing a copy of the best individual at the next time step. Because of symmetry reasons, let consider only the part of the ring at the right side of the connected region. The cell $k+2$ has a probability 1/2 to be contained in the set of cells after cell $k+1$ in the sweep, so it has a probability $(p/2)p$ to contain a copy of the best individual in the next time step. In general, a cell $k+j+1$ has a probability 1/2 to be after cell $k+j$ in the sweep, so it has a probability $(p/2)^j p$ to contain a copy of the best individual in the next time step. The recurrence describing the growth of the random variable $N(t)$ is, therefore

$$\begin{cases} N(0)=1 \\ E[N(t)]=\sum_{j=1}^{n} P[N(t-1)=j]\left(j+2\sum_{i=1}^{n-j} p\left(\frac{p}{2}\right)^{i-1}\right) \end{cases}$$

which can be transformed into the recurrence

$$\begin{cases} N(0)=1 \\ E[N(t)] = \sum_{j=1}^{n} P[N(t-1)=j]\ \left(j+4\sum_{i=1}^{n-j}\ \left(\frac{p}{2}\right)^i\right). \end{cases}$$

Since $\sum_{i=1}^{n-j}(p/2)^i$ is a geometric progression for large n, we can approximate this quantity by the limit value $p/(2-p)$ of the summation. The recurrence is, thus, equivalent to the following one:

$$\begin{cases} N(0)=1 \\ E[N(t)] = E[N(t-1)] + \frac{4p}{2-p}. \end{cases}$$

The closed form of the previous recurrence is

$$E[N(k)] = \frac{4p}{2-p}\, k+1$$

and we conclude that the expected takeover time for a fixed (or new) random sweep asynchronous cEA with a population of size n is

$$E[T] = \frac{2-p}{4p}\,(n-1).$$

D. Asynchronous Uniform Choice Takeover Time

To model takeover time for asynchronous uniform choice cEAs it is preferable to use cell update steps u instead of time steps in the recurrences. As for the other update policies, the region containing the copies of the best individual at update step u is a connected part of the ring $B(u) = \{l,\ldots,k\}$ (with $1 < l \leq k < n$). At each update step the two cells $l-1$ and $k+1$ have probability $1/n$ to be selected, and each cell has a probability p, if selected, to contain a copy of the best individual after the selection and the replacement phases. The recurrence describing the growth of the random variable $N(u)$, counting the number of copies of the best individual at update step u, thus, becomes

$$\begin{cases} N(0)=1 \\ E[N(u)] = \sum_{j=1}^{n} P[N(u-1)=j]\ \left(j+2\,\frac{1}{n}\,p\right) \end{cases}$$

which can be transformed into

$$\begin{cases} N(0)=1 \\ E[N(u)] = E[N(u-1)] + 2\,\frac{1}{n}\,p. \end{cases}$$

We can easily derive the closed form of the previous recurrence

$$E[N(u)] = \frac{2}{n}\,p\,u+1.$$

Since a time step is defined as n update steps, where n is the population size, the expected takeover time for a uniform choice asynchronous cEA in terms of time steps is

$$E[T] = \frac{1}{2p}\,(n-1).$$

We notice that the expected takeover time for a uniform choice asynchronous cEA is equal to the expected takeover time for a synchronous cEA.

It should be noted also that the present asynchronous uniform choice update model is very similar to what goes under the name of *nonlinear voter model* in the probability literature [22]. As well, it can be considered analogous to a steady-state cellular EA with a generation gap of $1/n$.

VII. Torus Structure

We consider cEAs defined on a square lattice of finite-size $\sqrt{n} \times \sqrt{n}$. The neighborhood we consider in this paper is the von Neumann neighborhood, which is constituted by a central

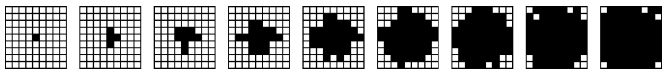

Fig. 3. Example of a probabilistic selection growth of $N(t)$ for a population of 81 individuals on a 9×9 torus structure.

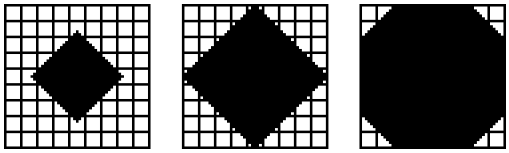

Fig. 4. Geometric approximation of a probabilistic selection growth in a torus structured population: a rotated square grows as a function of time, starting as an unrestricted growth until the square reaches the edges of the grid, and then saturating the population.

cell plus the four first neighbor cells in the directions north, east, south, and west [see Fig. 1(b)].

Because of the torus wrap-up properties, at each time step t the expected number of copies $N(t)$ of the best individual is independent from its initial position. Therefore, the expected takeover time is $E[T] = E_i[T], \forall i$.

We have seen in Section V the limiting case of the growth with a deterministic selection (i.e., a mechanism that selects the best individual in the neighborhood with probability $p = 1$). It should be noted that, in that case, the time variable t in the equations determines the measure of the half diagonal of the 45° rotated square (see Fig. 2). When modeling a probabilistic selection method, the exact recurrences, as derived for the ring topology in the previous section, become very complicated. In fact, as it can be seen in Fig. 3, the phenomenon that has to be modeled implies different selection probabilities in different locations in the grid.

Since we wanted to keep the models simple and easily interpretable, we decided to approximate the geometry of the propagation as the growth of a rotated square in the torus (see Fig. 4).

Using this geometric growth, we can approximate the measures of the side s and the half diagonal d of the 45° rotated square in the following way:

$$s = \sqrt{N(t)}, \quad d = \frac{\sqrt{N(t)}}{\sqrt{2}}.$$

With these quantities, in the next sections we will focus on synchronous and asynchronous takeover times, using the relevant probabilities in each case.

A. Synchronous Takeover Time

Let us consider the growth of such a region with a selection mechanism of probabilities p_1, p_2, p_3, p_4, and p_5 of selecting the best individual when there are, respectively, 1, 2, 3, 4, and 5 copies of it in the neighborhood.

Assuming that the region containing the copies of the best individual expands keeping the shape of a 45° rotated square, we can model the growth of $N(t)$ with the following recurrence:

$$\begin{cases} N(0) = 1 \\ N(t) = N(t-1) + 4p_2 \frac{\sqrt{N(t-1)}}{\sqrt{2}}, & \text{for } N(t) \leq \frac{n}{2} \\ N(t) = N(t-1) + 4p_2 \sqrt{n - N(t-1)}, & \text{for } N(t) > \frac{n}{2} \end{cases}.$$

It is practically impossible to find the closed analytical form of these recurrences, as it will be the case for the asynchronous models of the next sections. Therefore, we only give the explicit recurrences in each case.

B. Asynchronous Fixed Line Sweep Takeover Time

This update method, which is meaningful in a ring topology, in the case of a toroidal topology can be criticized. In fact, there is no biological parallelism for this update mechanism. A precise model for such update would be very complicated, since it is difficult to approximate the shape of the region containing the copies of the best individual. We have, therefore, decided to keep the model simple and understandable, to roughly approximate the shape of the region with a square stretched to the southeast direction, growing with probability p_1 on the northeast side, p_2 on the southeast side, and p_1 in the south direction.

Let us suppose that in any line the cells containing a copy of the best individual at time step t have index l to k. In the next time step, the cell $l-1$ will contain a copy of the best individual with probability p, while the cells $k+j$ (with $j = 1, \ldots, n-s$) will contain a copy of the best individual with probability p^j. The number of copies of the best individual in the considered line in the next time step is

$$p + \sum_{i=1}^{\sqrt{n}-j} p^i.$$

For large n, we can approximate this quantity by the limit $(2p - p^2)/(1-p)$. Therefore, we can model the growth of $N(t)$ with the following recurrence shown in the equation at the bottom of the page.

C. Asynchronous Fixed and New Random Sweep Takeover Time

The behaviors of fixed random sweep and new random sweep averaged over all the possible permutations of the individuals on the grid are equivalent also in the toroidal case. We, therefore, give only one model describing the growth of the random variable $N(t)$ for both policies.

In one time step, following the geometrical approximation, the probability of one individual on the border of the region being taken over by the best is p_2, while an individual at distance 2 from the region can be replaced by the best if one or two of its

$$\begin{cases} N(0) = 1 \\ N(t) = N(t-1) + \left(\frac{2p_2 - p_2^2}{1-p_2} + 2\frac{2p_1 - p_1^2}{1-p_1} \right) \sqrt{N(t-1)}, & \text{for } N(t) \leq \frac{n}{2} \\ N(t) = N(t-1) + \left(\frac{2p_2 - p_2^2}{1-p_2} + 2\frac{2p_1 - p_1^2}{1-p_1} \right) \sqrt{n - N(t-1)}, & \text{for } N(t) > \frac{n}{2} \end{cases}$$

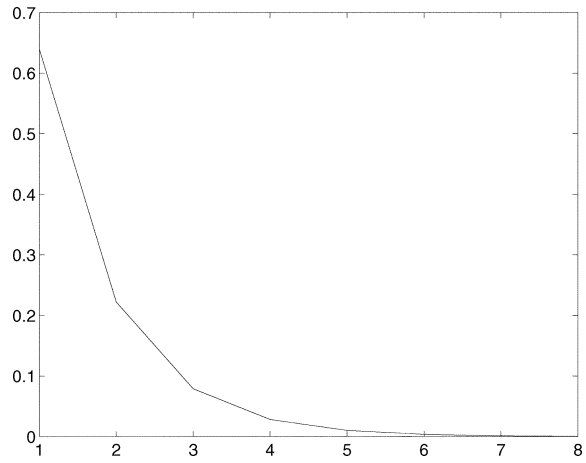

Fig. 5. Probability of an individual being replaced by a copy of the best individual (y axis) with respect to distance (x axis) from the region formed by copies of the best for asynchronous fixed (and new) random sweep. Note that the curve is traced continuously for clarity but the probability is calculated only at discrete points.

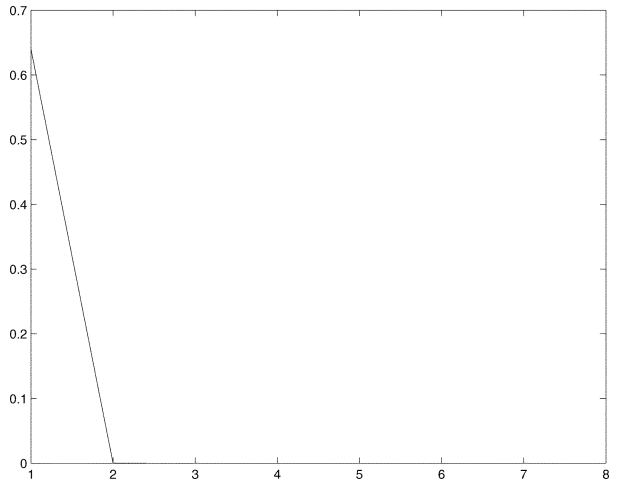

Fig. 6. Probability of an individual being replaced by a copy of the best individual (y axis) with respect to distance (x axis) from the region formed by copies of the best for uniform choice. Probability is discrete but the curve is continuous for clarity.

neighbors have already been replaced during the sweep. One of its neighbors is replaced if:

- only one neighbor comes before in the sweep (and it has been replaced);
- two neighbors come before in the sweep but just one has been replaced.

Two of its neighbors are replaced if the two come before in the sweep and the two have been replaced. The average probability for a couple of individuals of being before one another in a sweep is 1/2; therefore, an individual at distance 2 from the region is replaced with probability

$$2\left(\frac{1}{2}\left(1-\frac{1}{2}\right)p_2p_1\right)+2\left(\frac{1}{2}\frac{1}{2}p_2(1-p_2)p_2\right)+\frac{1}{2}\frac{1}{2}p_2^2p_2=$$
$$=p_2p_1+\frac{1}{4}(p_2-2p_1)p_2^2.$$

At distance 3 or more of the same reasoning can be done, but we have decided to model the growth up to distance 2 because, as it can been seen in Fig. 5, the probability at distances≥ 3 becomes negligible.

Thus, we can model the growth of $N(t)$ with the following recurrence, as shown in the first equation at the bottom of the page.

D. Asynchronous Uniform Choice Takeover Time

The ways in which an individual can be replaced in a time step for this update case are the same as for fixed and new random sweep (see before). In the present case, the average probability of an individual coming before a given other individual in a time step is $1/n$; therefore, an individual at distance 2 from the region is replaced with probability

$$\frac{1}{n}p_2p_1+\frac{1}{n^2}(p_2-2p_1)p_2^2.$$

The probability is already very small at distance 2 (see Fig. 6). Thus, in our model we only take into account individuals at distance 1 from the region.

In terms of time steps, the growth of $N(t)$ can be modeled with the following recurrence, as shown in the second equation at the bottom of the page.

VIII. Experimental Validation

In this section, we provide a set of validation tests intended to demonstrate the accuracy of the developed mathematical models. Since cEAs are good candidates for using selection methods that are easily extensible to small local pools, we use binary tournament and linear ranking in our experiments. Fitness-proportionate selection could also be used but it suffers

$$\begin{cases} N(0)=1 \\ N(t)=N(t-1)+4\left(p_2p_1+\frac{1}{4}(p_2-2p_1)p_2^2\right)\left(\sqrt{N(t-1)}-1\right)+4p_1, & \text{for } N(t)\leq\frac{n}{2} \\ N(t)=N(t-1)+4\left(p_2p_1+\frac{1}{4}(p_2-2p_1)p_2^2\right)\left(\sqrt{n-N(t-1)}-1\right)+8p_3, & \text{for } N(t)>\frac{n}{2} \end{cases}$$

$$\begin{cases} N(0)=1 \\ N(t)=N(t-1)+4p_2\sqrt{N(t-1)}, & \text{for } N(t)\leq\frac{n}{2} \\ N(t)=N(t-1)+4p_2(\sqrt{n-N(t-1)}-1)+8p_3, & \text{for } N(t)>\frac{n}{2} \end{cases}$$

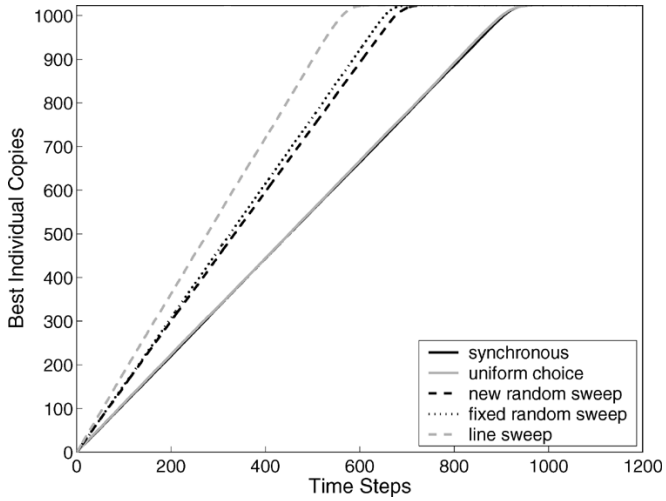

Fig. 7. Takeover times with binary tournament selection: mean values over 100 runs. The vertical axis represents the number of copies $N(t)$ of the best individual in each population as a function of the time step t. Synchronous and UC curves are superposed (rightmost curves).

from stochastic errors in small populations (e.g., at a neighborhood level), and it is more difficult to model theoretically since it requires knowledge of the fitness distribution function.

We have used the binary tournament selection mechanism described by Rudolph [17]: two individuals are randomly chosen with replacement in the neighborhood of a given cell, and the one with the better fitness is selected for the replacement phase.

In linear ranking selection the individuals in the neighborhood of a considered cell are ranked according to their fitness: each individual then has probability

$$\frac{2(s-i)}{(s(s-1))}$$

to be selected for the replacement phase, where s is the number of cells in the neighborhood and i is its rank in the neighborhood.

A. Ring Structure

For this study the cEA structure has a ring topology of size 1024 with neighborhood of radius 1. Only the selection operator is active: for each cell it selects one individual in the cell neighborhood (the cell and its two adjacent cells situated at its right and left). The selected individual replaces the old individual only if it has a better fitness.

1) Binary Tournament Selection: Fig. 7 shows the experimental growth curves of the best individual for the synchronous and the four asynchronous update methods. We can notice that the mean curves for the two asynchronous fixed and new random sweep show a very similar behavior. The graph also shows that the asynchronous update methods give an emergent selection pressure greater than that of the synchronous case, growing from the uniform choice to the line sweep, with the fixed and new random sweep in between.

The numerical values of the mean takeover times for the five update methods, along with their standard deviations, are shown in Table I, where it can be seen that the fixed random sweep and new random sweep methods give results that are statistically indistinguishable, and can therefore be described by a single model, as we assumed in Section VI-C. The same can be said for the synchronous and the uniform choice methods, as our models predicted.

TABLE I
MEAN ACTUAL TAKEOVER TIME AND STANDARD DEVIATION OF THE TOURNAMENT SELECTION FOR THE FIVE UPDATE METHODS. MEAN VALUES OVER 100 INDEPENDENT RUNS

	Synchro	LS	FRS	NRS	UC
Mean Takeover Time	925.03	569.82	666.18	689.29	920.04
Standard Deviation	20.36	24.85	17.38	20.27	26.68

Since we use a neighborhood of radius 1, at most one individual with the best fitness will be present in the neighborhood of a considered cell, except for the last update when there are two of them. It turns out that the probability for an individual having a copy of the best individual in its neighborhood to select it is $p = 5/9$. Using this probability in the models described in Section III, we calculated the theoretical growth curves. Fig. 8 shows the predicted and the experimental curves for the five update methods, and the mean-square error (mse) between them.

Looking at the curves, and taking into account the small value of the mse, it is clear that the models faithfully predict the observed takeover times. Moreover, the equivalence between new random sweep and fixed random sweep, as well as that of synchronous and uniform choice are fully confirmed.

2) Linear Ranking Selection: Fig. 9 shows the experimental growth curves of the best individual for the synchronous and the four asynchronous update methods. We can observe in the linear ranking case the same behavior that previously emerged in the binary tournament case: the mean curves for the synchronous and the asynchronous uniform choice cases are superposed, and the mean curves for the two asynchronous fixed and new random sweep show very similar behaviors. The graph shows that the asynchronous update methods give an emergent selection pressure greater than that of synchronous one, growing from the uniform choice to the line sweep, with the fixed and new random sweep in between.

The numerical values of the mean takeover times for the five update methods, along with their standard deviations, are shown in Table II. Again, the results show that the two random sweep methods are statistically equivalent, which is also the case for the synchronous and uniform choice methods.

With this linear ranking selection method, a cell having a copy of the best individual in its neighborhood has a probability $p = 2/3$ of selecting it. Using this value in the models described in Section III, we can calculate the theoretical growth curves. Fig. 10 shows the predicted and the experimental curves for the five update methods, and the mse between them. As it can be seen, the agreement between theory and experiment is excellent.

B. Torus Structure

We now describe the validation of the models for the torus structure in the same conditions that we used for the ring topology. The cEA structure has torus topology of size 32×32

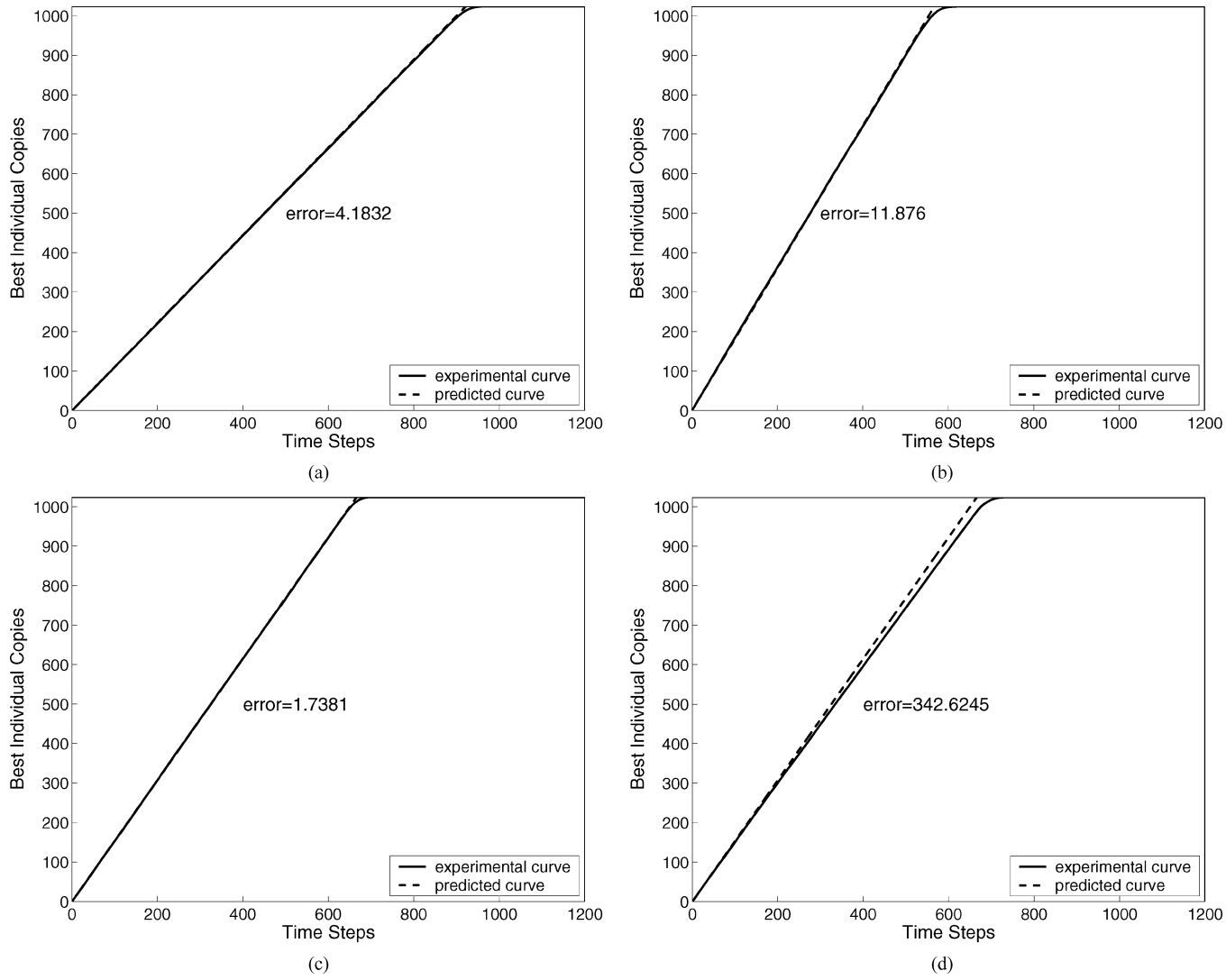

Fig. 8. Comparison of the experimental takeover time curves (full) with the model (dashed) in the case of binary tournament selection for four update methods. (a) Synchronous. (b) Asynchronous line sweep. (c) Asynchronous fixed random sweep. (d) Asynchronous new random sweep. Asynchronous uniform choice gives the same curve as the synchronous update, therefore, it is omitted. In each figure, the mse between the predicted and the actual curves is shown.

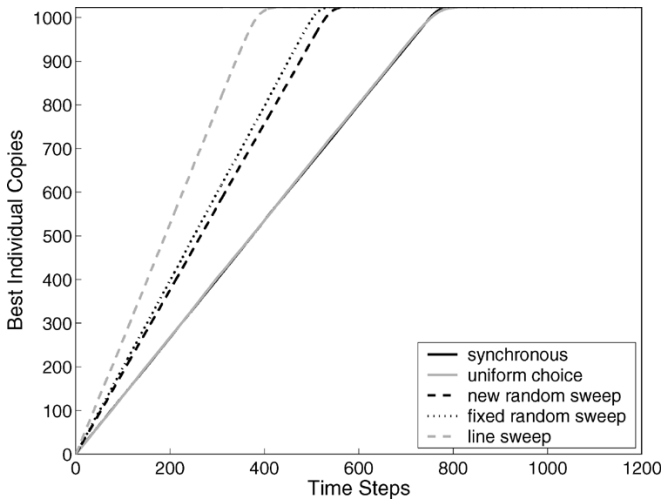

Fig. 9. Takeover times with linear ranking selection: mean values over 100 runs. The vertical axis represents the number of copies $N(t)$ of the best individual in each population as a function of the time step t. Synchronous and UC curves are superposed (rightmost curves).

TABLE II
MEAN TAKEOVER TIME AND STANDARD DEVIATION OF THE LINEAR RANKING SELECTION FOR THE FIVE UPDATE METHODS. MEAN VALUES OVER 100 INDEPENDENT RUNS

	Synchro	LS	FRS	NRS	UC
Mean Takeover Time	768.04	387.09	519.92	541.14	766.5
Standard Deviation	17.62	19.21	14.26	14.48	25.44

with von Neumann neighborhood. Only the selection operator is active: for each cell it selects one individual in the cell neighborhood, and the selected individual replaces the old individual only if it has a better fitness. This study is addressed separately for the two selection methods, binary tournament and linear ranking, in the forthcoming two sections.

1) Binary Tournament Selection: Fig. 11 shows the growth curves of the best individual for the panmictic, the synchronous, and three asynchronous update methods. In all cases the same set of parameters has been used. The mean curves for the two asynchronous methods, fixed and new random sweep, show a very similar behavior, so we have decided to plot only the new

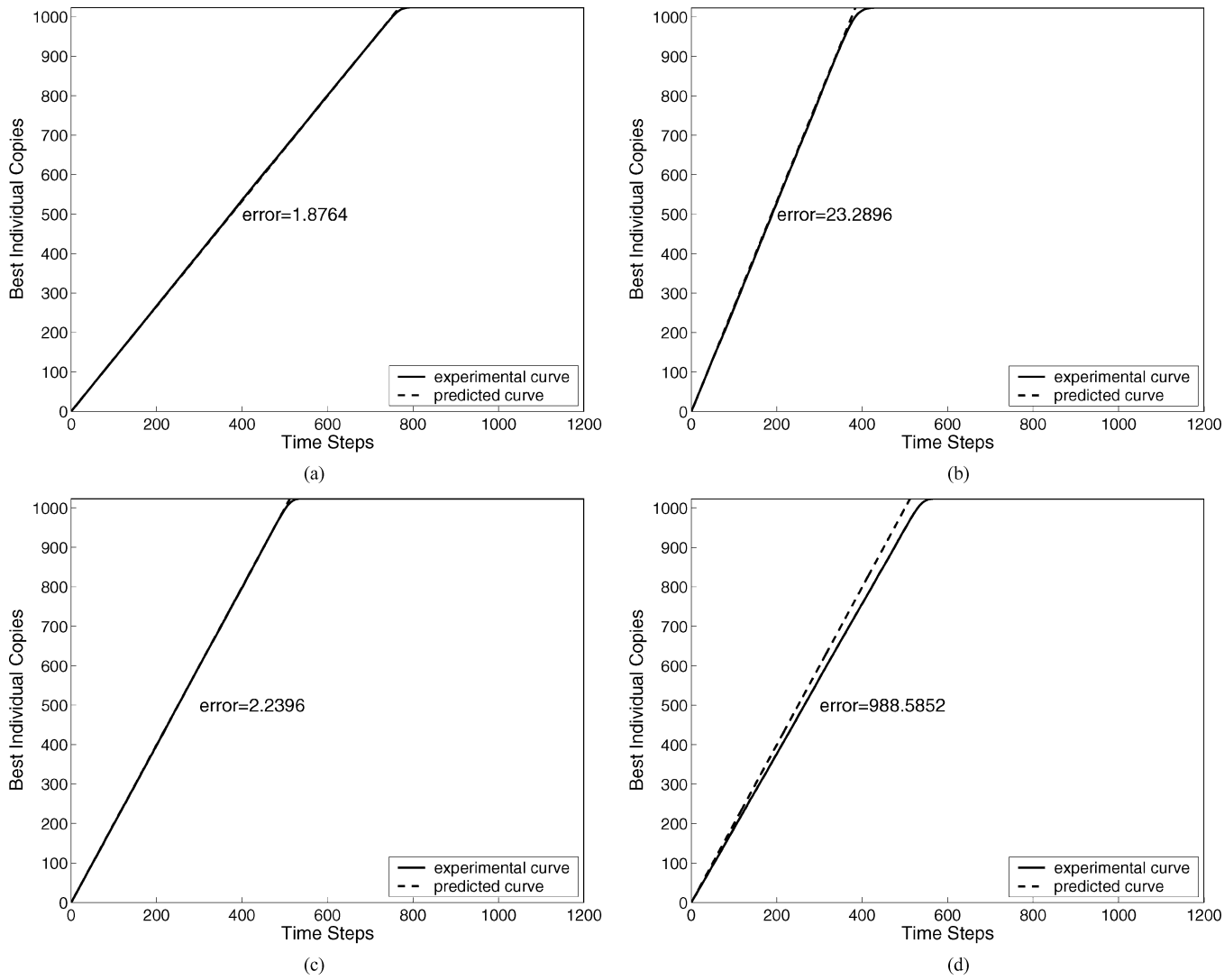

Fig. 10. Comparison of the experimental takeover time curves (full) with the model (dashed) in the case of linear ranking selection for four update methods. (a) Synchronous. (b) Asynchronous line sweep. (c) Asynchronous fixed random sweep . (d) Asynchronous new random sweep. Asynchronous uniform choice gives the same curve as the synchronous update, therefore, it is omitted. In each figure, the mse between the predicted and the actual curves is shown.

random sweep results. The graph shows that the asynchronous update methods give an emergent selection pressure greater than that of the synchronous case, growing from the uniform choice to the line sweep, with the fixed and new random sweep in between (similar to our findings for the ring topology).

The numerical values of the mean takeover times for the five update methods, together with their standard deviations are shown in Table III, where it can be seen that the fixed random sweep and new random sweep methods give results that are statistically indistinguishable. However, this time the differences between the uniform choice and the synchronous update are meaningful in a torus.

Since we use a von Neumann neighborhood, the probabilities p_1, p_2, and p_3 of selecting the best individual when there are, respectively, 1, 2, and 3 copies of it in the neighborhood are, respectively, 9/25, 16/25, and 21/25. Using these probabilities in the models, we calculated the theoretical growth curves. Fig. 12 shows the predicted and the experimental curves for the five update methods. It can be observed that the agreement between

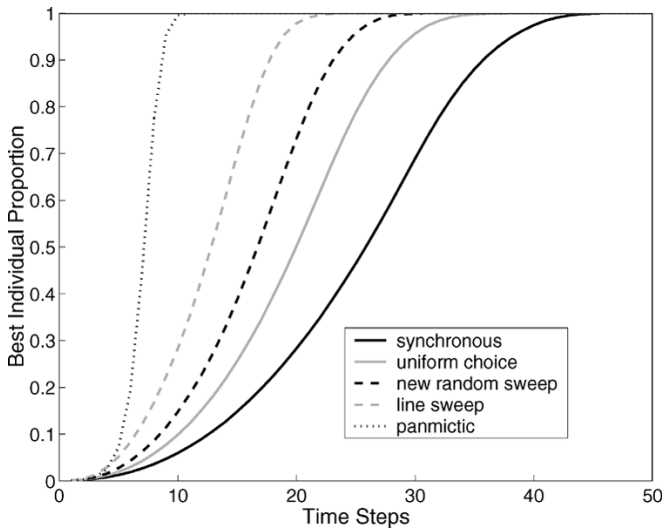

Fig. 11. Takeover times with binary tournament selection. Mean values over 100 runs. The vertical axis represents the number of copies $N(t)$ of the best individual in each population as a function of the time step t.

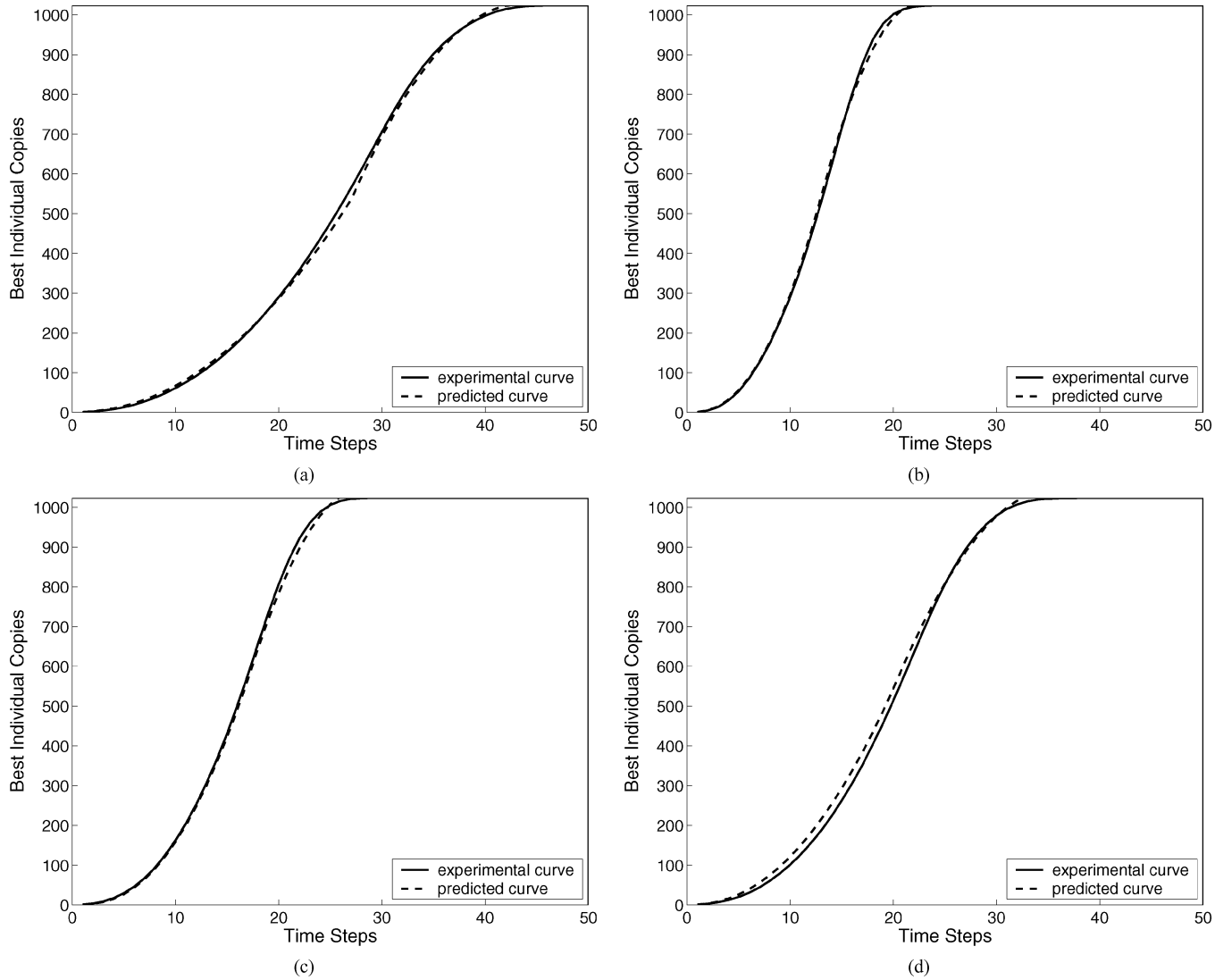

Fig. 12. Comparison of the experimental takeover time curves (full) with the model (dashed) in the case of binary tournament selection for four update methods. (a) Synchronous. (b) Asynchronous line sweep. (c) Asynchronous fixed random sweep. (d) Uniform choice.

theory and experiment is very good, in spite of the approximations made in the models.

2) Linear Ranking Selection: Fig. 13 shows the growth curves of the best individual for the panmictic, the synchronous, and three asynchronous update methods, using the same parameter set in all cases. We can observe in the linear ranking case the same behavior that emerged in the binary tournament case: the average curves for the two asynchronous updates, fixed and new random sweep, show a very similar behavior. We have, therefore, decided to plot only the new random sweep results. The graph shows that the asynchronous update methods give an emergent selection pressure greater than that of synchronous one, growing from the uniform choice to the line sweep, with the fixed random sweep in between. The numerical values of the mean takeover times for the five update methods, together with their standard deviations are shown in Table IV. Again, the results show that the two random sweep methods are statistically equivalent, while the uniform choice and synchronous are not.

Since we use a von Neumann neighborhood, the probabilities p_1, p_2, and p_3 of selecting the best individual when there are,

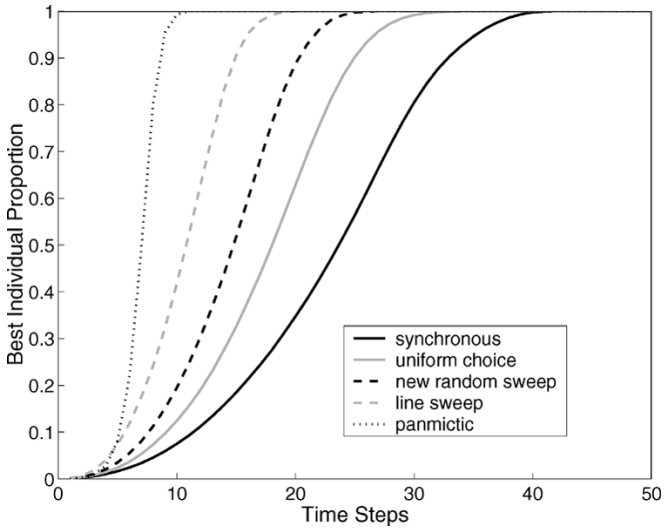

Fig. 13. Takeover times with linear ranking. Mean values over 100 runs. The vertical axis represents the number of copies $N(t)$ of the best individual in each population as a function of the time step t.

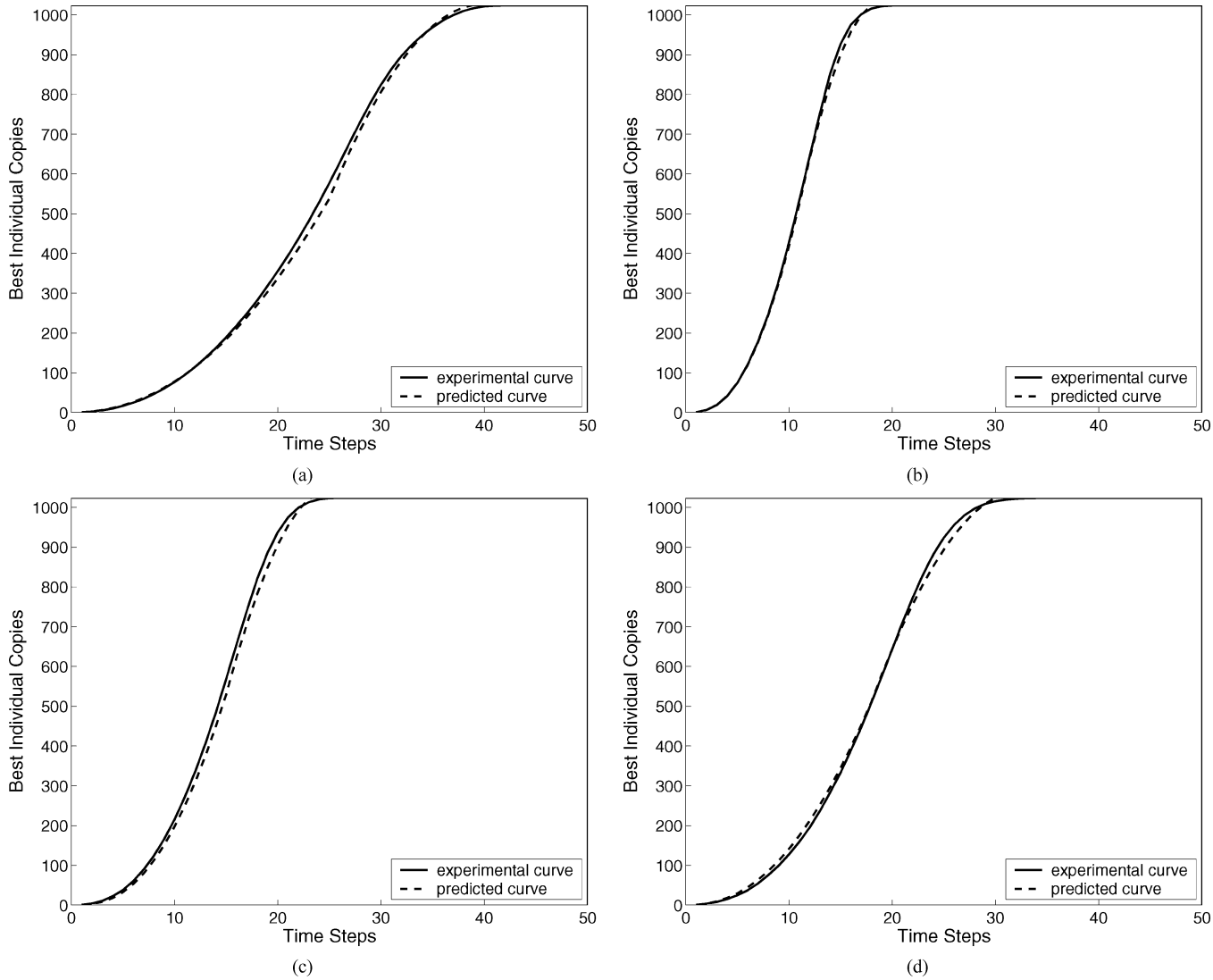

Fig. 14. Comparison of the experimental takeover time curves (full) with the model (dashed) in the case of linear ranking selection for four update methods. (a) Synchronous. (b) Asynchronous line sweep. (c) Asynchronous fixed random sweep. (d) Uniform choice.

TABLE IV
MEAN TAKEOVER TIME AND STANDARD DEVIATION OF THE LINEAR RANKING SELECTION FOR THE FIVE UPDATE METHODS. MEAN VALUES OVER 100 INDEPENDENT RUNS

	Synchro	LS	FRS	NRS	UC
Mean Takeover Time	40.68	18.2	23.96	24.89	32.16
Standard Deviation	1.2703	1.633	1.4766	1.4626	2.3856

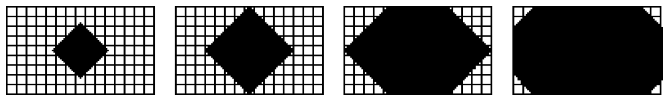

Fig. 15. Geometric approximation of a probabilistic selection growth in a rectangular toroidal structured population.

respectively, 1, 2, and 3 copies of it in the neighborhood are, respectively, 2/5, 7/10, and 9/10. Using these probabilities in the models, we calculated the theoretical growth curves. Fig. 14 shows the predicted and the experimental curves for the five update methods. The agreement between theory and experiment can be considered very good.

IX. RECTANGULAR TOROIDAL STRUCTURES

It has been shown in the literature [3], [23] that varying the ratio of the grid axes in a 2-D cEA is another simple way for controlling the global induced selection pressure. In this section, we address with our models the prediction of takeover regimes for cEAs whose population shape is toroidal but not square. Since different kinds of rectangular shapes could be used in a toroidal cEA, we here analyze the behavior of the mathematical models in such scenarios.

Let us suppose a rectangular toroidal structure of size equal to $a \times b$, with $a \geq b$; the same geometrical approximation, done in the case of a square toroidal structure (see Fig. 4), can be applied to this case. This time the models will describe the growth of a rotated square until its area is equal to $b^2/2$, followed by a composition of b linear growths until the area of the region is $ab - b^2/4$, plus a final quadratic saturation (see Fig. 15).

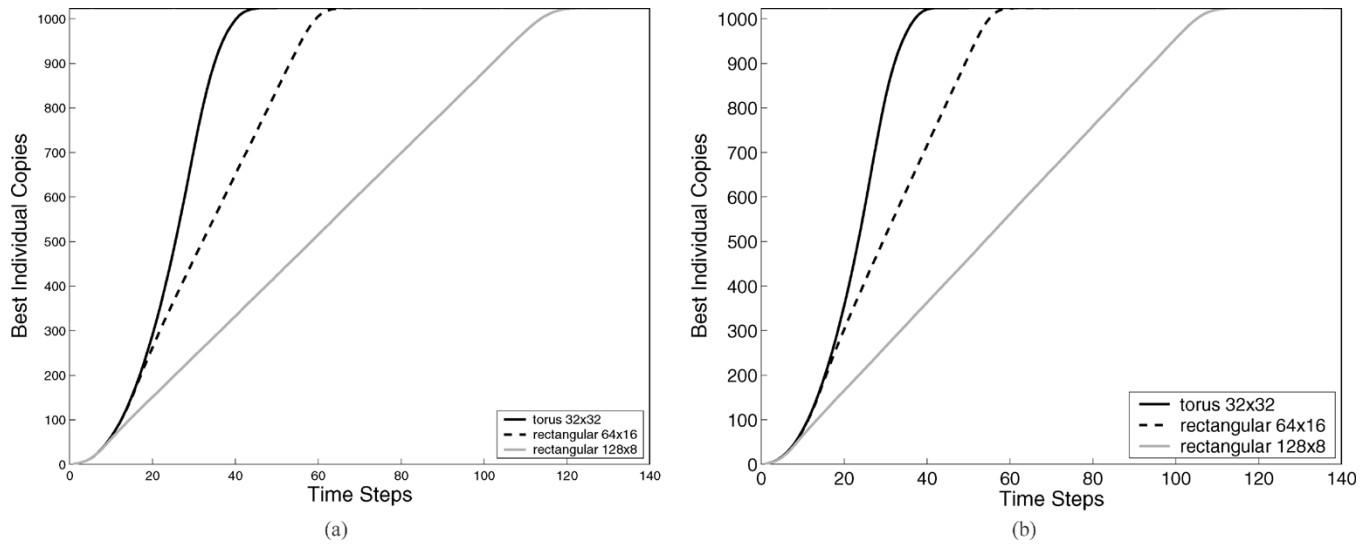

Fig. 16. Growth curves of synchronous evolutions on toroidal structures with different axis sizes using (a) binary tournament selection, and (b) linear ranking selection.

The recurrences modeling the synchronous and the three asynchronous evolutions will, therefore, be composed by the initial condition ($N(0) = 1$), followed by the equation describing the unrestricted growth of the square (until $N(t) = b^2/2$), then the composition of b linear growths (until $N(t) = ab - b^2/4$), and finally, the saturation equation.

For a synchronous evolution the recurrences are

$$\begin{cases} N(0) = 1 \\ N(t) = N(t-1) + 4p_2 \frac{\sqrt{N(t-1)}}{\sqrt{2}} \\ N(t) = N(t-1) + 2(b-1)p_2 + p_1 \\ N(t) = N(t-1) + 4p_2\sqrt{n - N(t-1)} \end{cases}.$$

For an asynchronous fixed line sweep update the model is

$$\begin{cases} N(0) = 1 \\ N(t) = N(t-1) + \left(\frac{2p_2 - p_2^2}{1-p_2} + 2\frac{2p_1 - p_1^2}{1-p_1}\right)\sqrt{N(t-1)} \\ N(t) = N(t-1) + \left(\frac{2p_2 - p_2^2}{1-p_2}\right)(b-1) + \frac{2p_3 - p_3^2}{1-p_3} \\ N(t) = N(t-1) + \left(\frac{2p_2 - p_2^2}{1-p_2} + 2\frac{2p_1 - p_1^2}{1-p_1}\right)\sqrt{ab - N(t-1)} \end{cases}.$$

For asynchronous fixed and new random sweeps updates the recurrences are shown in the equation at the bottom of the page. For asynchronous uniform choice evolutions the model is

$$\begin{cases} N(0) = 1 \\ N(t) = N(t-1) + 4p_2\sqrt{N(t-1)} \\ N(t) = N(t-1) + 2\sqrt{2}p_2(b-1) + p_1 \\ N(t) = N(t-1) + 4p_2(\sqrt{ab - N(t-1)} - 1) + 8p_3 \end{cases}.$$

As it was the case for the models of the square toroidal structure, also for these recurrences the closed analytical form of the recurrences is practically impossible to be derived.

TABLE V
MEAN TAKEOVER TIME WITH STANDARD DEVIATION IN PARENTHESIS OF THE BINARY TOURNAMENT SELECTION FOR THE FIVE UPDATE METHODS ON THE 64×16 AND THE 128×8 RECTANGULAR TOROIDAL TOPOLOGIES. MEAN VALUES OVER 100 INDEPENDENT RUNS

	Synchro	LS	FRS	NRS	UC
64×16	62.15 (2.4)	29.99 (2.3)	38.1 (1.9)	39.37 (2.0)	48.96 (2.9)
128×8	117.07 (3.7)	55.37 (4.2)	70.57 (3.3)	73.26 (3.5)	89.48 (4.3)

TABLE VI
MEAN TAKEOVER TIME WITH STANDARD DEVIATION IN PARENTHESIS OF THE LINEAR RANKING SELECTION FOR THE FIVE UPDATE METHODS ON THE 64×16 AND THE 128×8 RECTANGULAR TOROIDAL TOPOLOGIES. MEAN VALUES OVER 100 INDEPENDENT RUNS

	Synchro	LS	FRS	NRS	UC
64×16	57.42 (2.1)	24.6 (2.2)	33.89 (2.1)	35.3 (1.9)	45.05 (2.9)
128×8	108.32 (3.1)	45.98 (3.5)	62.69 (2.6)	64.76 (3.0)	80.78 (4.6)

A. Rectangular Toroidal Models Validation

The cEA structures have now rectangular torus topologies of sizes 64×16 and 128×8 with von Neumann neighborhood. On the two topologies the cEA has been run, as in the previous experiments, using the binary tournament and the linear ranking selections. The results (summarized in Table V for the binary tournament and in Table VI for the linear ranking) show a similar behavior as the one observed in the ring and torus topologies. In fact, to the synchronous updates always corresponds the greater takeover time, and the four asynchronous evolutions takeover times are ranked with the fixed line sweep being the faster, the uniform choice the slowest and the fixed and new random sweeps, that are statistically indistinguishable in between.

$$\begin{cases} N(0) = 1 \\ N(t) = N(t-1) + 4\left(p_2 + p_2p_1 + \frac{1}{4}(p_2 - 2p_1)p_2^2\right)\left(\sqrt{N(t-1)} - 1\right) + 4\left(p_1 + p_1^2 + \frac{1}{4}(p_2 - 2p_1)p_1^2\right) \\ N(t) = N(t-1) + \frac{4p_2}{2-p_2}(b-1) + \frac{4p_1}{2-p_1} + \frac{4p_3}{2-p_3} \\ N(t) = N(t-1) + 4\left(p_2 + p_2p_1 + \frac{1}{4}(p_2 - 2p_1)p_2^2\right)\left(\sqrt{ab - N(t-1)} - 1\right) + 8\left(p_3 + p_3p_1 + \frac{1}{4}(p_3 - 2p_1)p_3^2\right) \end{cases}$$

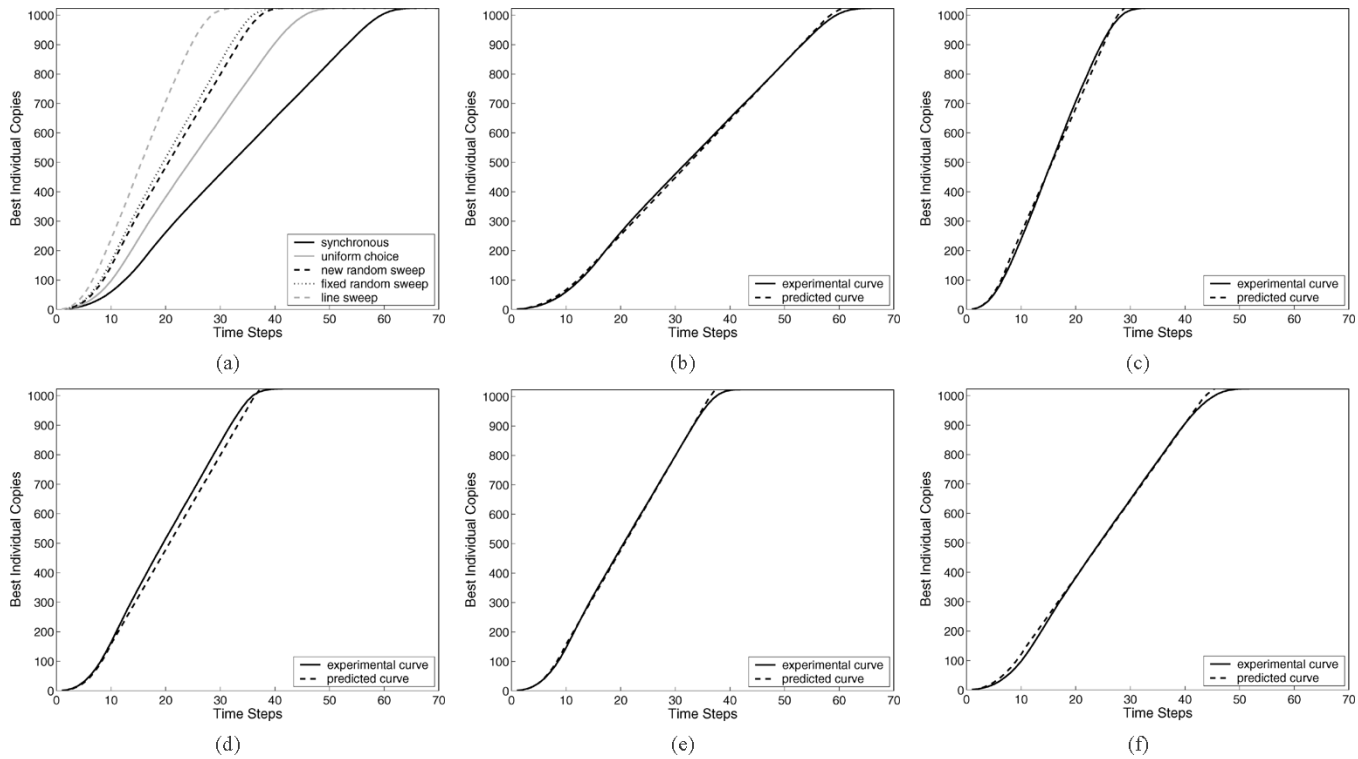

Fig. 17. (a) Experimental curves for rectangular 64×16 with binary tournament. Comparison of the experimental takeover time curves (full) with the model (dashed) in the case of linear ranking selection for four update methods. (b) Synchronous. (c) Asynchronous line sweep. (d) Asynchronous fixed random sweep. (e) Asynchronous new random sweep. (f) Uniform choice.

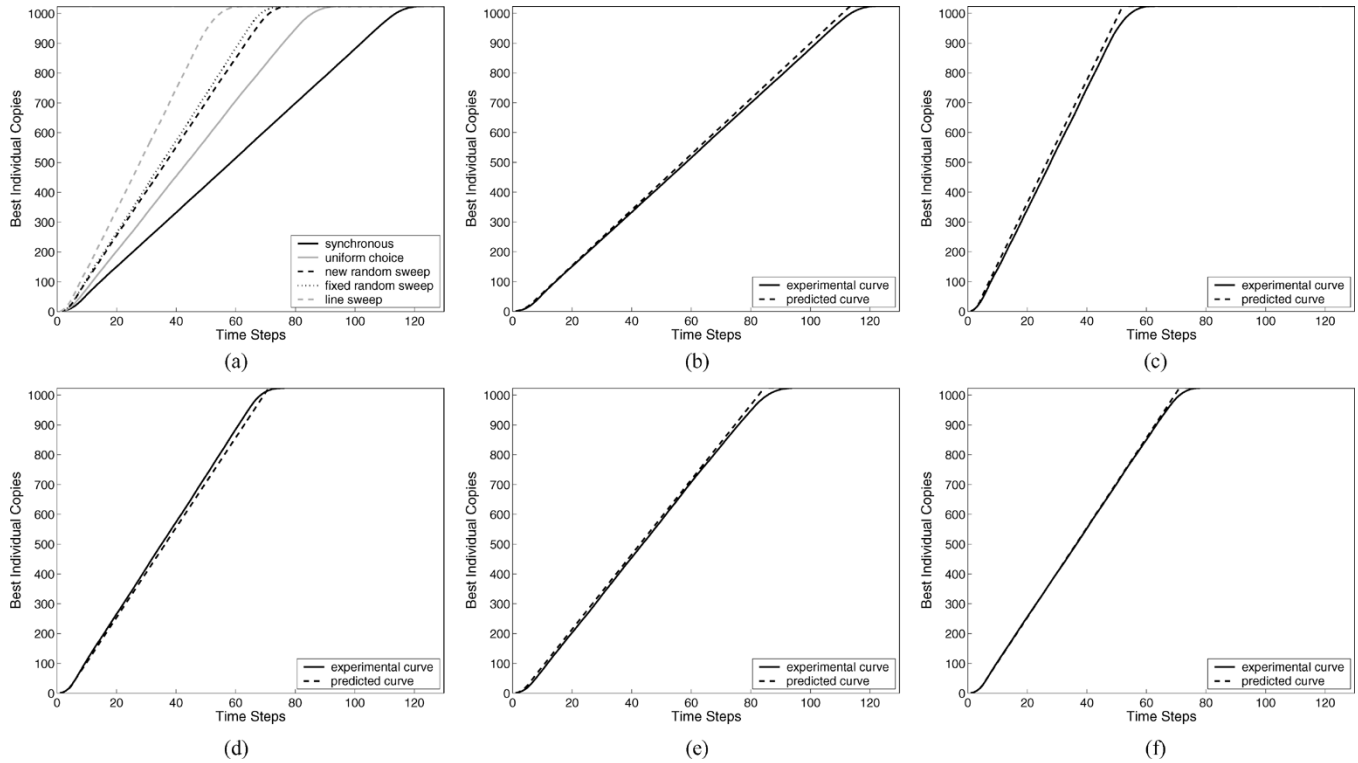

Fig. 18. (a) Experimental curves for rectangular 128×8 with binary tournament. Comparison of the experimental takeover time curves (full) with the model (dashed) in the case of linear ranking selection for four update methods. (b) Synchronous. (c) Asynchronous line sweep. (d) Asynchronous fixed random sweep. (e) Asynchronous new random sweep. (f) Uniform choice.

As expected, the selection pressure induced by the different sizes of the grids reduces as the grid gets thinner [3], [23]. Fig. 16 shows the different growth curves that result in changing the grid axis values from those of a square to a thin rectangle, when using the binary tournament and the linear ranking selection schemes.

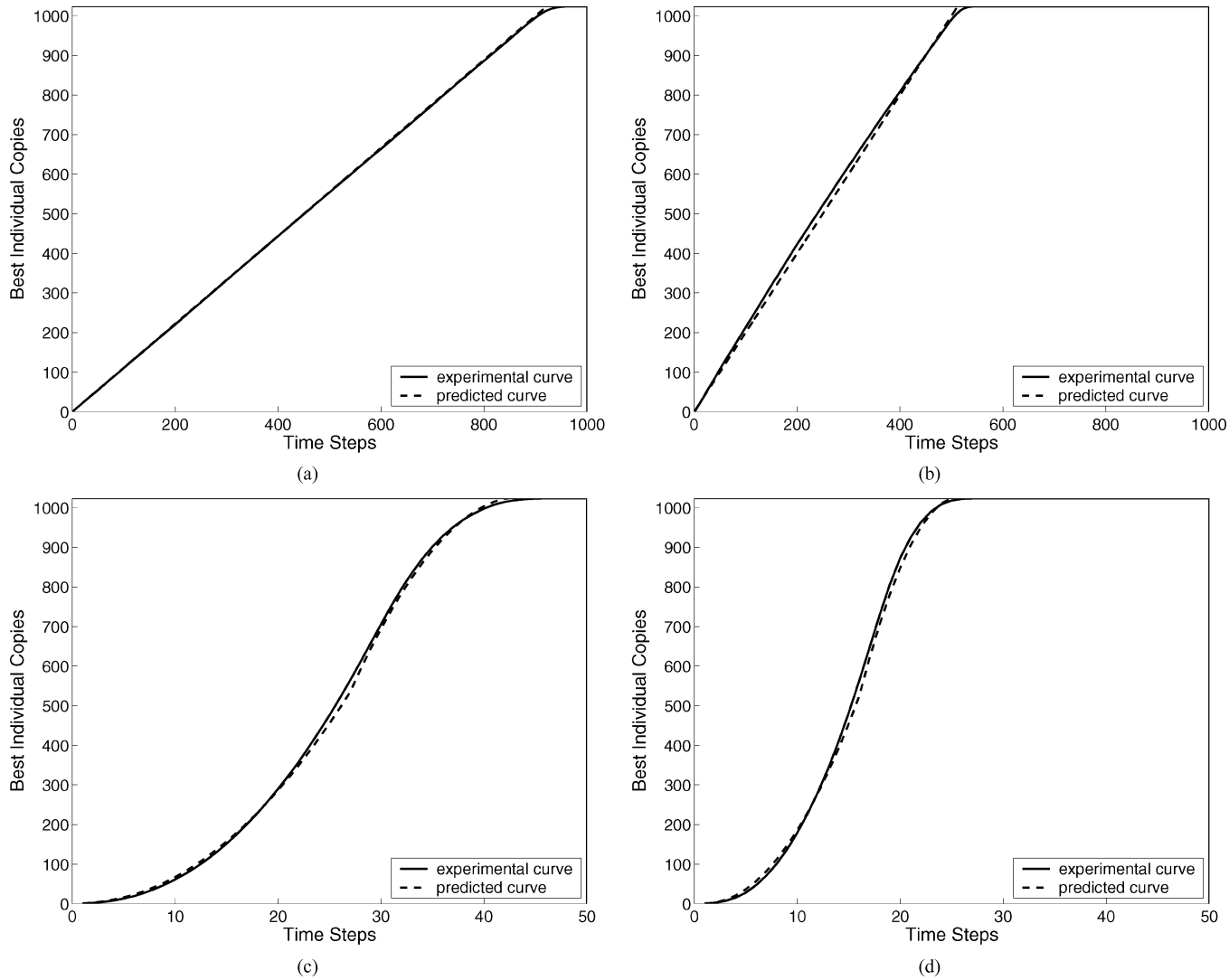

Fig. 19. Comparison of the experimental takeover time curves (full) with the model (dashed) in the case of binary tournament selection for synchronous in case of a ring with (a) radius 1 and (b) radius 2 neighborhoods, and in a torus with (c) radius 1 and with (d) radius 2 generalized von Neumann neighborhoods.

As it can be seen in Figs. 17 and 18, the models successfully predict the experimental curves. When using linear ranking selection, the accuracy of the models is comparable, therefore, we decided not to show the relative graphs.

X. Varying the Radius

Sarma and De Jong have shown convincingly that the neighborhood's size and shape have an important influence on the induced global selection pressure in the grids [6], [7]. For this reason, and to complete our study, in this section, we turn to change the basic value for the radius used until now. We, therefore, use generalized von Neumann neighborhood of radius 2 in both 1-D and 2-D regular lattices. Such neighborhood is defined as containing all the individual at distance smaller or equal to the radius, where the Manhattan distance is used on the 2-D grid.

The equation for a ring with radius 2 is as follows:

$$\begin{cases} N(0) = 1 \\ N(1) = N(0) + 4p_1 \\ N(t) = N(t-1) + 2p_2 + 2p_1 \end{cases}$$

where p_i is the probability that a copy of the best individual is selected when i copies of it are present in the neighborhood.

On the other hand, if we use the same geometrical approximation described in Section VII, the model equations for a torus with a radius 2 generalized von Neumann neighborhood is shown in the equation at the top of the next page, where p_i is the probability that a copy of the best individual is selected when i copies of it are present in the neighborhood.

The two previous models have been tested using a binary tournament selection mechanism: the comparisons between the predicted and the actual curves are shown in Fig. 19. The models are still accurate, and could be extended to generalized von Neumann neighborhoods with larger radii.

Although this is not apparent from the explicit recurrences, looking at the curves one can infer that when the radius tends to $n/2$ in the ring case, and when radius tends to $\sqrt{n}$ in the grid case, then the curves tend to the panmictic limit.

XI. Concluding Remarks

In this paper, we offer a set of mathematical models that predict the growth curves and the takeover time regime and value

$$\begin{cases} N(0) = 1 \\ N(1) = N(0) + 12p_1 \\ N(t) = N(t-1) + 4p_5\frac{\sqrt{N(t-1)}}{\sqrt{2}} + 4p_3\frac{\sqrt{N(t-1)}+1}{\sqrt{2}} + +2p_1\frac{\sqrt{N(t-1)}+2}{\sqrt{2}}, & \text{for } N(t) \leq \frac{n}{2} \\ N(t) = N(t-1) + 4p_5(\sqrt{n - N(t-1)}) + +4p_3(\sqrt{n - N(t-1)} - 2) + 2p_1(\sqrt{n - N(t-1)} - 2), & \text{for } N(t) > \frac{n}{2} \end{cases}$$

for a broad range of cEAs on regular lattices. We consider ring, as well as toroidal topologies, both under tournament and linear ranking methods for selection in the neighborhood.

We have shown that basic logistic models cannot predict the actual behavior of these algorithms, and we propose difference equations that model observed growth curves in a highly accurate manner. To sustain our claims, we include detailed graphs of the errors, all of them proving excellent agreement between theory and practice. The similarities and differences between the ring and the toroidal models are discussed. In addition, the results show comparable behavior between the two selection methods under investigation.

Finally, we have mathematically explained the global induced selection pressure when a nonsquare topology is used in toroidal cEAS, an important factor describing their performance. Just in the same line, different radius values are studied to offer a complete work on this topic.

The main observation, already noted before by several researchers, is that the selection intensity in the population is lower in lattices than in panmictic populations. We have also seen that different asynchronous policies give rise to significantly different global emergent selection pressures and can, thus, be used to control the explorative or exploitative character of the algorithm to some extent, without resorting to ad hoc tricks in selection methods.

Another way that can be used to control the selection intensity in cEAs is through the size and shape of the neighborhood or, in the 2-D case, by statically or dynamically adapting the ratio of the grid axes, with "flatter" rectangular shapes giving lower global pressures [24].

As future research, it could be useful to find out the implications of using fitness proportionate selection mechanisms. It would also be worthwhile to study possible extensions of the logistic models that could fit the actual selection curves as accurately as the offered models do in this work, but with simpler analytical forms.

REFERENCES

[1] M. Gorges-Schleuter, "ASPARAGOS an asynchronous parallel genetic optimization strategy," in *Proc. 3rd Int. Conf. Genetic Algorithms*, J. D. Schaffer, Ed., 1989, pp. 422–427.

[2] B. Manderick and P. Spiessens, "Fine-grained parallel genetic algorithms," in *Proc. 3rd Int. Conf. Genetic Algorithms*, J. D. Schaffer, Ed., 1989, pp. 428–433.

[3] B. Dorronsoro, E. Alba, M. Giacobini, and M. Tomassini, "The influence of grid shape and asynchronicity on cellular evolutionary algorithms," in *Proc. Congr. Evol. Comput.*, 2004, pp. 2152–2158.

[4] E. Alba and M. Tomassini, "Parallelism and evolutionary algorithms," *IEEE Trans. Evol. Comput.*, vol. 6, no. 5, pp. 443–462, Oct. 2002.

[5] G. Folino, C. Pizzuti, and G. Spezzano, "A scalable cellular implementation of parallel genetic programming," *IEEE Trans. Evol. Comput.*, vol. 7, no. 1, pp. 37–53, Feb. 2003.

[6] J. Sarma and K. A. De Jong, "An analysis of the effect of the neighborhood size and shape on local selection algorithms," in *Lecture Notes in Computer Science*, H. M. Voigt, W. Ebeling, I. Rechenberg, and H. P. Schwefel, Eds. Berlin, Germany: Springer-Verlag, 1996, vol. 1141, Proc. Parallel Problem Solving From Nature—PPSN IV, pp. 236–244.

[7] ——, "An analysis of local selection algorithms in a spatially structured evolutionary algorithm," in *Proc. 7th Int. Conf. Genetic Algorithms*, T. Bäck, Ed., 1997, pp. 181–186.

[8] G. Rudolph and J. Sprave, "A cellular genetic algorithm with self-adjusting acceptance threshold," in *Proc. 1st IEE/IEEE Int. Conf. Genetic Algorithms Eng. Syst.: Innovations Applicat.*, London, U.K., 1995, pp. 365–372.

[9] M. Giacobini, M. Tomassini, and A. Tettamanzi *et al.*, "Modeling selection intensity for linear cellular evolutionary algorithms," in *Lecture Notes in Computer Science*, P. Liardet *et al.*, Eds. Berlin, Germany: Springer-Verlag, 2004, vol. 2936, Proc. 6th Int. Conf. Artif. Evol., pp. 345–356.

[10] M. Giacobini, E. Alba, A. Tettamanzi, and M. Tomassini *et al.*, "Modeling selection intensity for toroidal cellular evolutionary algorithms," in *Proc. Genetic Evol. Comput. Conf.*, K. Deb *et al.*, Eds., 2004, pp. 1138–1149.

[11] M. Giacobini, E. Alba, and M. Tomassini *et al.*, "Selection intensity in asynchronous cellular evolutionary algorithms," in *Proc. Genetic Evol. Comput. Conf.*, E. Cantú-Paz *et al.*, Eds., 2003, pp. 955–966.

[12] M. Tomassini, "The parallel genetic cellular automata: Application to global function optimization," in *Proc. Int. Conf. Artif. Neural Netw. Genetic Algorithms*, R. F. Albrecht, C. R. Reeves, and N. C. Steele, Eds., 1993, pp. 385–391.

[13] D. Whitley, "Cellular genetic algorithms," in *Proc. 5th Int. Conf. Genetic Algorithms*, S. Forrest, Ed., 1993, p. 658.

[14] R. Durrett, "Ten lectures on particle systems," in *Lectures on Probability Theory*, P. Biane and R. Durrett, Eds. Berlin, Germany: Springer-Verlag, 1995, vol. 1608, Lecture Notes in Mathematics, pp. 97–201.

[15] B. Schönfisch and A. de Roos, "Synchronous and asynchronous updating in cellular automata," *BioSystems*, vol. 51, pp. 123–143, 1999.

[16] D. E. Goldberg and K. Deb, "A comparative analysis of selection schemes used in genetic algorithms," in *Foundations of Genetic Algorithms*, G. J. E. Rawlins, Ed. San Mateo, CA: Morgan Kaufmann, 1991, pp. 69–93.

[17] G. Rudolph *et al.*, "On takeover times in spatially structured populations: Array and ring," in *Proc. 2nd Asia-Pacific Conf. Genetic Algorithms Applicat.*, K. K. Lai *et al.*, Eds., 2000, pp. 144–151.

[18] P. F. Verhulst, "Notice sur la loi que la population suit dans son acccroissement," *Corr. Math. et Phys.*, vol. 10, pp. 113–121, 1838.

[19] J. D. Murray, *Mathematical Biology, I: An Introduction*. Berlin, Germany: Springer-Verlag, 2002.

[20] P. Spiessens and B. Manderick, "A massively parallel genetic algorithm," in *Proc. 4th Int. Conf. Genetic Algorithms*, L. B. Booker and R. K. Belew, Eds., 1991, pp. 279–286.

[21] M. Gorges-Schleuter, "An analysis of local selection in evolution strategies," in *Proc. Genetic Evol. Conf.*, vol. 1, W. Banzhaf, J. Daida, A. E. Eiben, M. Garzon, V. Honavar, M. Jakiela, and R. Smith, Eds., 1999, pp. 847–854.

[22] R. Durrett, *Lecture Notes on Particle Systems and Percolation*. Belmont, CA: Wadsworth, 1988.

[23] E. Alba and J. M. Troya *et al.*, "Cellular evolutionary algorithms: Evaluating the influence of ratio," in *Lecture Notes in Computer Science*, M. Schoenauer *et al.*, Eds. Berlin, Germany: Springer-Verlag, 2000, vol. 1917, Parallel Problem Solving From Nature—PPSN VI, pp. 29–38.

[24] E. Alba and B. Dorronsoro, "The exploration/exploitation tradeoff in dynamic cellular genetic algorithms," *IEEE Trans. Evol. Comput.*, vol. 9, no. 2, pp. 126–142, Apr. 2005.

Mario Giacobini (S'05) received the Degree in mathematics from the University of Torino, Italy, in 1998, the M.S. degree in discrete mathematics and theoretical computer science from the University of Marseille, Marseille, France, in 2000, and the Ph.D. degree in computer science from the University of Lausanne, Lausanne, Switzerland, and the University of Milano, Milan, Italy.

He is currently working as a Research Assistant at the University of Lausanne and as an Invited Lecturer at the University of Torino. His current research interests are focused on the dynamics of the evolution of structured populations. He is also interested in artificial intelligence, and the modeling of complex biological networks. He has several publications in the above fields.

Marco Tomassini received the Degree in physical and chemical sciences from ICEI, Mendoza, Argentina, in 1969, and the Ph.D. degree in theoretical chemistry from the University of Perugia, Perugia, Italy, working on computer simulations of condensed matter systems.

He is a Professor of Computer Science at the Information Systems Department, University of Lausanne, Lausanne, Switzerland. He has been program chairman of several international events and has published many scientific papers and several authored and edited books in these fields. His current research interests are centered around the application of biological ideas to artificial systems. He is active in evolutionary computation, especially, spatially structured systems, genetic programming, and evolvable machines. He is also interested in machine learning, parallel cellular computing systems, and the dynamical properties of networked complex systems.

Andrea G. B. Tettamanzi received the Ph.D. degree in computational mathematics and operations research from the University of Milan, Crema, Italy, in 1995.

He is an Associate Professor at the University of Milan. In 1995, he was one of the founders of Genetica s.r.l., a Milan-based company specializing in applications of evolutionary computation. His research interests are in the field of evolutionary algorithms and soft computing, focusing on bridging the gap between theory and real-world applications.

Enrique Alba received the Ph.D. degree in designing and analyzing parallel and distributed genetic algorithms from the University of Málaga, Málaga, Spain, in 1999.

He is a Professor of Computer Science at the University of Málaga. He has published many scientific papers in international conferences and journals. His current research interests involve the design and application of evolutionary algorithms, neural networks, and other bioinspired systems to real problems including telecommunications, combinatorial optimization, and bioinformatics. The main focus of all his work is on parallelism.

Dr. Alba has received National and International Awards for his research results.